

# Ultrafast strong field quantum control on K<sub>2</sub> dimers

M. Wollenhaupt, T. Baumert\*

University of Kassel, Institute of Physics and Center for Interdisciplinary Nanostructure Science and Technology (CINSA<sup>T</sup>),  
Heinrich-Plett-Str. 40, D-34132 Kassel, Germany

Available online 18 April 2006

## Abstract

In this theoretical wave packet study, we demonstrate efficient strong field quantum control by Selective Population of Dressed States (SPODS) on K<sub>2</sub> dimers. Shaped femtosecond pulses are used to switch population transfer among different final states with high selectivity and almost unit efficiency. The physical mechanism of this ultrafast molecular strong field control scenario is analyzed in analogy to the interpretation of recent experimental studies of SPODS on atoms. Criteria for the design of SPODS-pulses are presented along with experimental signatures for the observation of SPODS on molecules.

© 2006 Elsevier B.V. All rights reserved.

**Keywords:** Multiphoton excitation; Quantum control; Intense laser fields; Dressed states; SPODS

## 1. Introduction

Current ultrashort pulse shaping techniques [1] offer unprecedented prospects for quantum control of photochemical reactions [2–7]. The general objective of laser control of photochemical reactions is to maximize the yield of specific products with high selectivity and high efficiency by design of suitably shaped laser pulses. The tools developed for quantum control of atomic and molecular dynamics by shaped ultrashort laser pulses have been successfully extended to large molecules in solution [8,9] comprising applications to photobiology [10]. Much work has been devoted to studies of weak field quantum control, i.e. control schemes in which the light matter interaction is treated perturbatively. However, from a microscopic perspective, maximizing the product yield is associated with efficient population transfer into a predefined target state implying non-perturbative depletion of the ground state population. Efficient population transfer can be achieved by strong field schemes operative on the nanosecond time scale such as Rapid Adiabatic Passage (RAP) and Stimulated Rapid Adiabatic Passage (STIRAP) [11]. However, another constraint for coherent quantum control of chemical and biological samples in solution is electronic decoherence on ultrashort time scales. To counteract decoherence effects, efficient population transfer needs to

be accomplished on the ultrashort time scale. This requirement is met by the use of *ultrashort* intense laser fields [12]. For example, control on the vibrational wave packet dynamics during the course the reaction was exerted by strong field induced level shifts [13,14]. Even faster switching among the different final states was achieved by control of the electronic coherence via Selective Population of Dressed States (SPODS). SPODS is based on techniques originally developed in NMR (spin locking) [15]. The optical analogue termed photon locking [16] was demonstrated experimentally using cw-excitation [17]. Applications of photon locking to molecules using complex shaped pulses was investigated theoretically [18]. Experimentally, *ultrafast* strong field control by SPODS using phase coherent double pulses was demonstrated on the photoelectron spectra of potassium atoms [19]. Subsequently, strong field quantum control via SPODS using pulse shaping techniques was investigated using sinusoidal spectral phase modulation [20,21], chirped excitation [22] and adaptive optimization of the spectral phase [23]. In view of applications to chemistry selectivity and tunability up to 2000 cm<sup>-1</sup> was demonstrated experimentally on atoms and the attainable control was studied on a molecular model system theoretically [21]. Implications to quantum optics were discussed in terms of the analogy to a temporal Young's double slit experiment in weak [24] and strong [23] laser fields.

In this contribution we will extend the principles of SPODS as experimentally observed on potassium atoms to real molecules in view of laser control of chemical reactions. Molecules are characterized by additional degrees of freedom such as vibra-

\* Corresponding author. Tel.: +49 561 804 4452.

E-mail address: [tbaumert@physik.uni-kassel.de](mailto:tbaumert@physik.uni-kassel.de) (T. Baumert).

tions and rotations. The effect of these further degrees of freedom is equivalent to a system characterized by many rovibronic states. Typically, the density of the electronic states increases rapidly with the electronic energy. Therefore it is not a priori clear whether SPODS as demonstrated in few level systems such as potassium atoms is operative under these conditions as well. Another challenge arises from the non-perturbative population transfer required for applications to chemical control. Unlike the scenario in potassium atoms where the photoelectrons act as spectators and could be treated by perturbation theory, for chemical control one is generally interested in non-perturbative population transfer—preferably with unit efficiency. However, non-perturbative interaction with the target states will affect the coherence properties of the intermediate states and might therefore reduce the efficiency of SPODS.

The paper is organized as follows. First we present the principle idea how SPODS is operative in quantum control of molecules. In order to apply these principles to a real molecule we consider the excitation scheme of  $K_2$  dimers. Then, the theoretical description of strong field induced wave packet dynamics on  $K_2$  is given. Results are discussed in terms of the temporal evolution of the population for specifically tailored pulses. In order to establish criteria for the design of optimal laser pulses, we investigate the final population as a function of the relative optical phase.

Fig. 1 illustrates schematically how SPODS is operative in controlling the final state population of a molecule during a multiphoton process. The light-induced reaction proceeds via the intermediate Potential Energy Surface (PES) A and two final PES B and C that are connected to the reaction channels I and II, respectively. Control is exerted by a shaped pulse which creates a coherent superposition of the ground and the A state within its leading edge. In the central part of the pulse the phase is tailored such that one of the dressed A states is selectively populated, for example the lower dressed A state as indicated in Fig. 1. Then, this state is resonant with the—in principle also dressed—B PES whereas the upper dressed A state is resonant with the C PES. In the illustrated case absorption of another photon leads therefore to selective population of the B PES resulting in the selective formation of the photo products I whereas the C state remains unpopulated. In this way the selectivity of the final state population—and hence the outcome of the reaction—is controlled by the selective population of the intermediate dressed A state. In addition, the exact resonance between the intermediate dressed A state and the final states can be tuned by the energy splitting  $\hbar\Omega$  as demonstrated experimentally on atoms.

## 2. Excitation scheme

In this paper we study strong field control on the multiphoton excitation of  $K_2$  dimers. Unlike the generic scenario shown in Fig. 1 in potassium dimers we consider three different final states ( $4^1\Sigma_g^+$ ,  $2^1\Pi_g$  and  $5^1\Sigma_g^+$ )—rather than only the two PES B and C. The  $K_2$  potentials and transition moments relevant to the multiphoton excitation at a wavelength of 830 nm have been calculated by a two-electron full configuration interaction method using effective core potentials (ECP) and core polar-

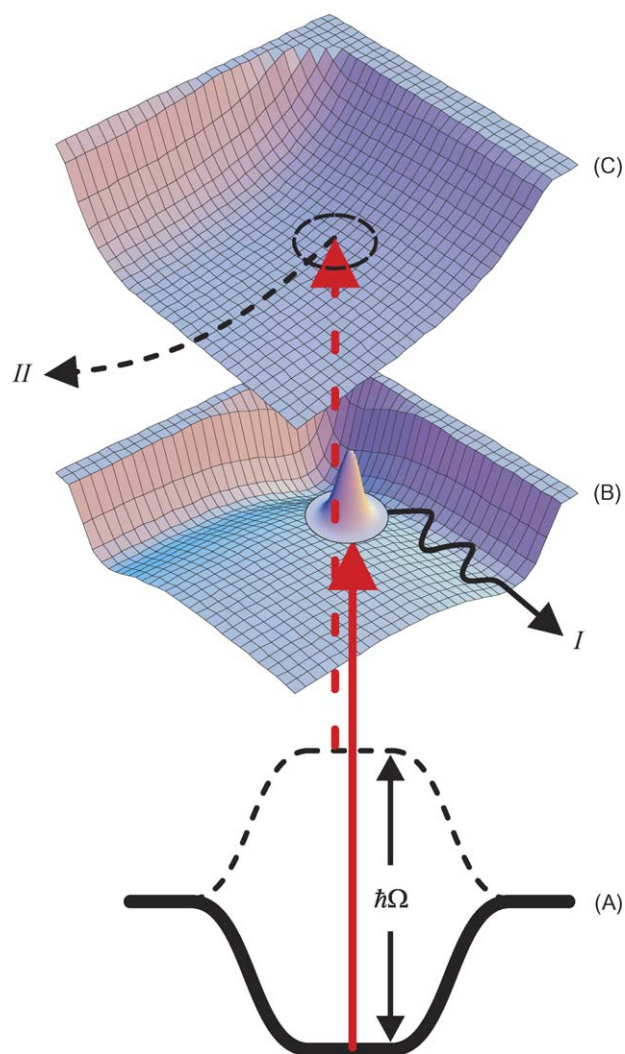


Fig. 1. Schematic illustration of the strong field control scenario for a multiphoton-induced chemical reaction with the possible outcomes I and II on two-dimensional Potential Energy Surfaces (PES) using SPODS. The intermediate A state is split into two dressed states due to the coherent interaction with an intense laser pulse. By phase control, only the lower dressed state is selectively populated (bold line). Since this state is shifted into resonance with the lower excited PES B a wave packet is selectively created on the B state leading to the selective formation of the photoproducts I. Selective population of the upper excited C state resulting in reaction channel II (not shown) is achieved by changing the relative phase of the second pulse by  $\pi$ .

ization potentials (CCP) [25], including a core–core interaction given by [26]. The same basis as in [27] was used, together with the ECP's form Ref. [28] and the CCP first proposed by Müller and Meyer [29]. This method has been proven to yield precise results for this system [27,30]. These potentials, together with the corresponding  $R$ -dependent transition dipole moments are shown in Fig. 2. It is also confirmed by experimental studies on alkali dimers that their electronic transitions are characterized by  $R$ -dependent dipole moments [31–34]. Therefore we take the  $R$ -dependent transition dipole moments into account in the description of the laser matter interaction. Because we will use pulses much shorter than the typical wave packet round trip times in the electronic states (e.g. about 370 fs for the  $X^1\Sigma_g^+$ -

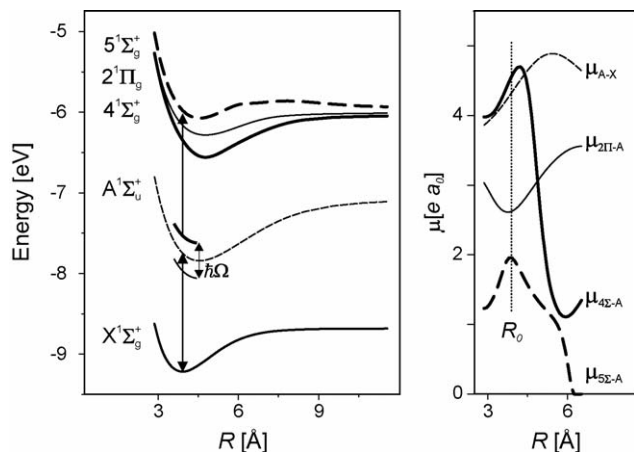


Fig. 2. Left: scheme for multiphoton excitation of potassium dimers  $K_2$ . The first part of the pulse creates a superposition state of the  $X^1\Sigma_g^+$  and the  $A^1\Sigma_u^+$  states. During the second part of the pulse the  $X^1\Sigma_g^+$  and the  $A^1\Sigma_u^+$  states are ‘photon locked’. The optical phase controls which of the dressed states (indicated at  $R_0$ ) energetically separated by  $\hbar\Omega$  is selectively populated. Absorption of another photon leads to population transfer to one of the (non-resonant) states  $4^1\Sigma_g^+$  and  $5^1\Sigma_g^+$ . Selective population of the upper dressed state with subsequent transition to the  $5^1\Sigma_g^+$ -state is illustrated. Right:  $R$ -dependent dipole moments for the respective transitions. The dipole moments  $\mu_{A-X}$  (dashed),  $\mu_{4\Sigma-A}$  (solid bold),  $\mu_{2\Pi-A}$  (solid thin) and  $\mu_{5\Sigma-A}$  (dashed bold) at the equilibrium internuclear separation  $R_0$  are seen at the intersection with the dotted line.

state and about 500 fs for the  $A^1\Sigma_u^+$ -state), the wave packets will not move significantly during the excitation process. Therefore, we are mainly interested in the molecular properties in the region of the equilibrium internuclear separation  $R_0 = 3.9 \text{ \AA}$  as indicated with the dotted line in Fig. 2 (right panel). The excitation scheme as indicated by the arrows in Fig. 2 (left panel) proceeds via vertical transitions from the  $X^1\Sigma_g^+$ -state via the  $A^1\Sigma_u^+$ -state to the higher excited states  $4^1\Sigma_g^+$ ,  $2^1\Pi_g$  and  $5^1\Sigma_g^+$ . At  $R_0$  both higher excited  $1^1\Sigma_g^+$ -states are separated from the  $2^1\Pi_g$ -state by approximately 185 meV. The ratios of the corresponding dipole moments  $\mu_{A-X}(R_0)$ ,  $\mu_{4\Sigma-A}(R_0)$ ,  $\mu_{2\Pi-A}(R_0)$  and  $\mu_{5\Sigma-A}(R_0)$  at the equilibrium internuclear separation are 2.2:2.3:1.3. In the simulation we start with the vibronic ground state wave function  $\Psi_{X,v''=0}$ . We first consider resonant perturbative excitation of  $K_2$  at 830 nm. Upon excitation, a wave packet is created in the  $A^1\Sigma_u^+$ -state. Although the  $A^1\Sigma_u^+(v' = 14)$  state is resonant at this wavelength, the wave packet is centered around the  $A^1\Sigma_u^+(v' = 11)$  state due to the Franck-Condon overlap. Absorption of a second photon leads to the creation of wave packets in higher electronic states. The  $4^1\Sigma_g^+$ -state is the lowest among these electronic states. Therefore at 830 nm this electronic state is always energetically accessible and highly vibrationally excited. Indeed, at this wavelength the vibrational states around the  $4^1\Sigma_g^+(v^* = 41) \leftarrow X^1\Sigma_g^+(v'' = 0)$  transition are approximately two-photon resonant. Two-photon resonant excitation of the energetically higher lying  $2^1\Pi_g$ -state leads to vibrational excitation centered at the  $2^1\Pi_g(v^* = 8)$  state. At 830 nm the higher lying  $5^1\Sigma_g^+$ -state is not (two-photon) energetically accessible from the  $X^1\Sigma_g^+(v'' = 0)$  state. For the transition  $5^1\Sigma_g^+(v^*) \leftarrow X^1\Sigma_g^+(v'' = 0)$  to occur photons at wavelengths below 790 nm are required.

### 3. Theoretical description

We describe the interaction of an intense phase coherent pulse sequence with potassium dimers by numeric solution of the time dependent Schrödinger equation. The light field consists of two overlapping pulses at a wavelength of  $2\pi c/\omega_0 = 830 \text{ nm}$  with equal full width at half maximum of  $\Delta t = 14.1 \text{ fs}$ . The pulse duration of 14.1 fs was chosen from local optimization of the final population starting at an experimentally accessible pulse duration of  $15 \pm 1 \text{ fs}$ . The second pulse is delayed with respect to the first by a delay time  $\tau$ . Decomposing the field  $\varepsilon(t)e^{i\omega_0 t}$  into the envelope and the carrier, the envelope  $\varepsilon(t)$  reads

$$\varepsilon(t) = \varepsilon_1(t) + \varepsilon_2(t) = E_1 e^{-2\ln 2(t/\Delta t)^2} + E_2 e^{-2\ln 2((t-\tau)/\Delta t)^2} e^{i\chi}, \quad (1)$$

where  $\chi = \omega_0 \tau$  describes the relative phase between both pulses determined by the delay.  $E_1$  and  $E_2$  characterize the peak electrical field of the pulses corresponding to an intensity of about  $4.2 \times 10^{10} \text{ W/cm}^2$  and  $6.8 \times 10^{11} \text{ W/cm}^2$  for the first and second pulse, respectively. As a consequence of the temporal overlap of both pulses the absolute value of the individual pulses  $|\varepsilon_1(t)|$  and  $|\varepsilon_2(t)|$  can temporarily exceed the absolute value of the coherent superposition of both  $|\varepsilon|$  due to (partially) destructive interference as depicted in Fig. 3. Since orthogonal transition dipole moment vectors  $\mu$  are involved in the multiphoton excitation of the highly excited states via the respective  $\Sigma \leftarrow \Sigma$  and  $\Pi \leftarrow \Sigma$  transitions, for simplicity, we assume the laser radiation to be polarized at  $\theta = 45^\circ$  with respect to the internuclear axis of an aligned molecular sample. Although, recently the vectorial character of the dipole moments in  $K_2$  was exploited for quantum control using polarization shaping [35], this particular aspect of the dynamics is deferred to a later study. Accounting for the effect of random orientation of the molecules within the sample requires an angular averaging procedure which is also deferred to a later study. In the simulation, the vibrational wave functions  $\psi_i(R, t)$  of the near resonant potentials shown in Fig. 2 are used to describe the state vector

$$\psi(R, t) = (\psi_X(R, t), \psi_A(R, t), \psi_{4\Sigma}(R, t), \psi_{2\Pi}(R, t), \psi_{5\Sigma}(R, t)). \quad (2)$$

Initially, i.e. before the light matter interaction, potassium atoms are in the vibronic ground state

$$\psi(R, -\infty) = (\Psi_{X,v''=0}(R), 0, 0, 0, 0), \quad (3)$$

where  $\Psi_{X,v''=0}(R)$  describes the lowest vibrational eigenstate in the  $X^1\Sigma_g^+$ -potential. The Hamiltonian of the system  $H = T + V(R, t)$  consists of the kinetic operator  $T$  and the potential operator  $V(R, t)$  including the light matter interaction terms  $V_{\text{rad}}(t)$ . The light field couples the  $X^1\Sigma_g^+$  and  $A^1\Sigma_u^+$ -states via the dipole moment  $\mu_{A-X}(R)$  and the  $A^1\Sigma_u^+$ -state with the  $4^1\Sigma_g^+$ ,  $2^1\Pi_g$  and  $5^1\Sigma_g^+$  states via the respective dipole moments  $\mu_{4\Sigma-A}(R)$ ,  $\mu_{2\Pi-A}(R)$  and  $\mu_{4\Sigma-A}(R)$ . Within the dipole approximation for the light matter interaction  $V_{\text{rad}}(t) = -\mu\varepsilon(t)$ , we obtain  $-\mu\varepsilon(t)\cos(\theta)$  for the parallel  $\Sigma \leftarrow \Sigma$  transitions and  $-\mu\varepsilon(t)\sin(\theta)$  for the perpendicular  $\Pi \leftarrow \Sigma$  transitions. By mak-

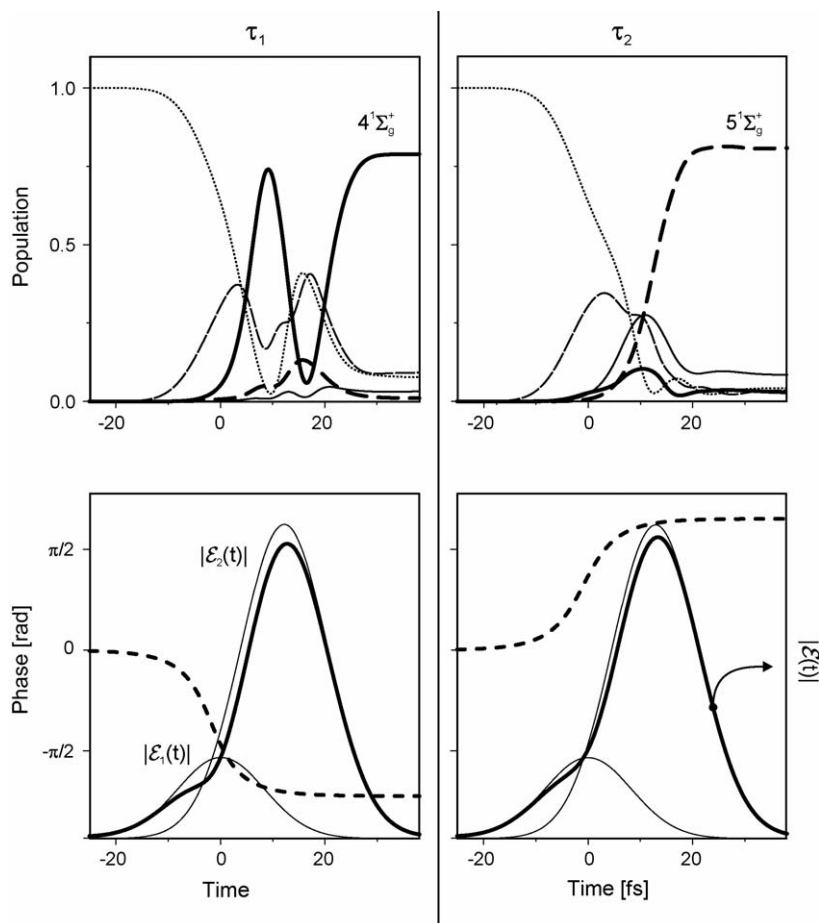


Fig. 3. Upper panels: time evolution of the population in the  $X^1\Sigma_g^+$ -state (dotted), the  $A^1\Sigma_u^+$ -state (dashed thin), the  $4^1\Sigma_g^+$ -state (bold solid), the  $2^1\Pi_g$ -state (solid thin) and the  $5^1\Sigma_g^+$ -state (dashed bold). Lower panels: absolute value of the envelope of the shaped laser pulse  $|\varepsilon(t)|$  (bold) and temporal phase function  $\chi(t)$  (dashed). The absolute values of the individual pulses  $|\varepsilon_i(t)|$  generating the sequence (thin solid) slightly exceed the coherent superposition due to (partially) destructive interference. The left and right panels correspond to a delay of  $\tau_1 = 12.1$  fs and  $\tau_2 = 12.9$  fs, respectively. At a delay of  $\tau_1$  ( $\tau_2$ ) the lower (upper, cf. Fig. 2) dressed state is populated leading to resonant excitation of the  $4^1\Sigma_g^+$ -state ( $5^1\Sigma_g^+$ -state) with 79% (81%) efficiency.

ing use of the rotating wave approximation the potential operator  $V(R, t)$  reads

$$\begin{pmatrix} V_X(R) & -\frac{\mu_{A-X}\varepsilon(t)}{2} & 0 & 0 & 0 \\ -\frac{\mu_{A-X}\varepsilon^*(t)}{2} & V_A(R) - \hbar\omega_0 & -\frac{\mu_{4\Sigma-A}\varepsilon(t)}{2} & -\frac{\mu_{2\Pi-A}\varepsilon(t)}{2} & -\frac{\mu_{5\Sigma-A}\varepsilon(t)}{2} \\ 0 & -\frac{\mu_{4\Sigma-A}\varepsilon^*(t)}{2} & V_{4\Sigma}(R) - 2\hbar\omega_0 & 0 & 0 \\ 0 & -\frac{\mu_{2\Pi-A}\varepsilon^*(t)}{2} & 0 & V_{2\Pi}(R) - 2\hbar\omega_0 & 0 \\ 0 & -\frac{\mu_{5\Sigma-A}\varepsilon^*(t)}{2} & 0 & 0 & V_{5\Sigma}(R) - 2\hbar\omega_0 \end{pmatrix}. \quad (4)$$

The time evolution of the state vector  $\psi(R, t)$  is obtained by iteratively solving time dependent Schrödinger equation employing a grid based representation of the wave functions propagated in time by a Fourier based split-operator method as for instance described in [36,4]. Checks of the numerical performance of our scheme comprise the reproduction of experimental [37–40] and theoretical [27,30] spectroscopic results as well as dynamical studies reported in [41,42].

#### 4. Results and discussion

The strong field induced dynamic is described in the picture of SPODS similar to the discussion of SPODS as observed experimentally on atoms [12,19–23]. Other descriptions in terms of light-induced potentials as for instance reported in [43–45]

are also possible. However, since the interpretation in terms of SPODS is straightforward, predictive and permits the design of tailored ultrashort laser pulses, we restrict ourselves to this description here.

We analyze the excitation mechanism using the pulse sequence described by Eq. (1) for two delay times  $\tau_1 = 12.1$  fs and  $\tau_2 = 12.9$  fs. To this end the time evolution of the population  $\langle \psi_i(R,t) | \psi_i(R,t) \rangle$  is plotted in Fig. 3 for all potentials  $V_i(R)$  involved. We start the discussion with the situation encountered at  $\tau_2 = 12.9$  fs (cf. Fig. 2 for a schematic representation and Fig. 3, right panels for the quantitative results). Although the pulses strongly overlap in time, for clarity, we will refer to the dynamics as being induced by a first and a second pulse. In the leading edge of the first pulse ( $\varepsilon_2(t)$ ) the resonant  $A^1\Sigma_u^+$  state is efficiently populated. Both energetically accessible highly excited states ( $2^1\Pi_g$  and  $4^1\Sigma_g^+$ ) are also populated during this time interval. With the onset of the second pulse (at around  $-10$  fs) the phase of the field changes to eventually converge to a value slightly above  $\pi/2$  at the end of the sequence. In the trailing edge of the first pulse at around 10 fs a coherent superposition of the  $X^1\Sigma_g^+$ -state and the  $A^1\Sigma_u^+$ -state with approximately equal population in both states is created. As the field of the second pulse starts exceeding the field of the first pulse (at around 0 fs) the upper dressed state starts being selectively populated (cf. Fig. 2). The strong second laser pulse ( $\varepsilon_2(t)$ ) introduces level shifts in the order of 200 meV in agreement with the separation of the potentials at  $R_0$  of about 185 meV. Hence, the upper dressed state is shifted into resonance with higher lying  $5^1\Sigma_g^+$ -state which was energetically inaccessible in the bare state representation of the potentials. As a consequence, population is transferred from the coherent superposition state to the  $5^1\Sigma_g^+$ -state. Since the other highly excited states ( $2^1\Pi_g$  and  $4^1\Sigma_g^+$ ) are no longer (strong field) resonant, population is pumped out of these states. After the pulse sequence 81% of the population remains in the  $5^1\Sigma_g^+$ -state whereas only 3% of the population arrive at the  $4^1\Sigma_g^+$ -state. In effect, this pulse sequence acts like a  $5^1\Sigma_g^+$ -state selective  $\pi$ -pulse. An experimental demonstration of a molecular  $2\pi$ -pulse was reported on the  $\text{Na}_2$  dimer [46,33].

The time evolution leading to selective population of the  $4^1\Sigma_g^+$ -state is shown in the left panels of Fig. 3. By changing the delay to  $\tau_1 = 12.1$  fs the relative phase between the two pulses converges to slightly below  $-\pi/2$ . In this case the maximum coherence between the  $X^1\Sigma_g^+$ -state and the  $A^1\Sigma_u^+$ -state is already attained at around 0 fs. Due to the phase change of approximately  $-\pi/2$  during the second pulse the lower dressed state is selectively populated. Now, the  $4^1\Sigma_g^+$ -state is in resonance with the populated lower dressed state leading to efficient population transfer to the  $4^1\Sigma_g^+$ -state. Because the dipole moment for the transition  $4^1\Sigma_g^+ \leftarrow A^1\Sigma_u^+$  is approximately twice the dipole moment for the transition  $5^1\Sigma_g^+ \leftarrow A^1\Sigma_u^+$ , i.e.  $\mu_{4\Sigma-A}(R_0) \approx 2.3\mu_{5\Sigma-A}(R_0)$ , Rabi oscillations in the  $4^1\Sigma_g^+$ -state population are observed. In the trailing edge of the second pulse the population of the other states decreases such that after the light matter interaction 79% of the population is stored in the  $4^1\Sigma_g^+$ -state whereas only 3% of the population arrive at the  $5^1\Sigma_g^+$ -state. In accordance with the larger dipole moment

the pulse sequence acts like a  $4^1\Sigma_g^+$ -state selective  $2.5\pi$ -pulse. These results show, that by controlling the temporal phase of the laser pulse during the light matter interaction we can switch the final population among different molecular states on the ultrashort time scale with high selectivity keeping all other molecular states essentially unpopulated.

In order to establish criteria for the design of SPODS-pulses, we investigate the final population of the highly excited states as a function of relative phase between the pulses. To this end wave packet calculations as shown in Fig. 3 for  $\tau_1 = 12.1$  fs and  $\tau_2 = 12.9$  fs have been performed for various delay times ranging from approximately 8 to 20 fs. The final population of the  $4^1\Sigma_g^+$ ,  $2^1\Pi_g$ - and  $5^1\Sigma_g^+$ -states is plotted in Fig. 4 for strong field excitation (upper panel) and perturbative excitation (lower panel). For reference we will first describe the results obtained by weak field excitation. Depending on the time delay, the energetically accessible states, i.e. the  $4^1\Sigma_g^+$ -state (bold line in Fig. 4) or the  $2^1\Pi_g$ -state (thin line in Fig. 4) are perturbatively excited. In the weak field limit selectivity is obtained via spectral interference, i.e. the delay-dependent modulation of the (multiphoton) spectrum of a pulse sequence, as for instance reported for atoms [47–49] and molecules [50–52]. Consequently, the  $5^1\Sigma_g^+$ -state remains unpopulated for all delay times because there is no overlap of the (modulated)  $2\omega$ -spectrum with the vibrational states of the  $5^1\Sigma_g^+$  potential. A very different picture arises when strong laser fields are used. Due to the above mentioned light-induced level shifts in the order of  $2000\text{ cm}^{-1}$  the (two-photon) energetically forbidden  $5^1\Sigma_g^+$ -state is efficiently populated for suitable delay times, i.e. suitable relative optical phases. In addition, the resonant  $2^1\Pi_g$ -state remains essentially unpopulated

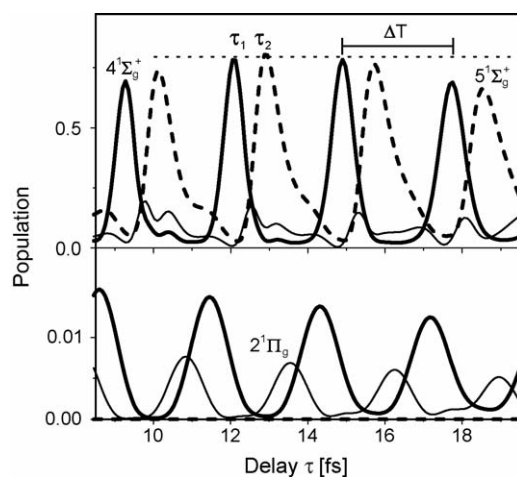


Fig. 4. Final population in the  $4^1\Sigma_g^+$ -state (bold), the  $2^1\Pi_g$ -state (solid thin) and the  $5^1\Sigma_g^+$ -state (dashed bold) as a function of the delay  $\tau$  within the pulse sequence for strong field excitation (upper panel) and perturbative excitation (lower panel). The delay time for selective excitation of the  $4^1\Sigma_g^+$ -state ( $\tau_1 = 12.1$  fs) and the  $5^1\Sigma_g^+$ -state ( $\tau_2 = 12.9$  fs) as shown in Fig. 3 are indicated. The dotted line indicates 80% population transfer. Selective excitation of a single final state is repeatedly obtained at the optical period of  $\Delta T = 2\pi/\omega_0 = 2.77$  fs. Because the  $5^1\Sigma_g^+$ -state is energetically not accessible at 830 nm, this state remains unpopulated in the weak field case. Note the phase shift between the weak and the strong field cases.

at all delay times. In the strong field case selectivity among the highly excited  $\Sigma$ -states is obtained via SPODS. Because the relative optical phase between the two pulses – which determines selective population of the upper or lower dressed state – is controlled by the delay  $\chi = \omega_0 \tau$ , switching between different final states occurs within one optical period  $\Delta T = 2\pi/\omega_0$ . However, the efficiency of the process is not constant at all the optimal delay times. For low delay times the pulses interfere such that the phase jump is not as distinct as for  $\tau_1$  and  $\tau_2$ . At larger delay times the motion of the wave packet weakens the effect of photon locking between the  $X^1\Sigma_g^+$  and the  $A^1\Sigma_u^+$  states.

From the above theoretical findings we conclude signatures of SPODS on molecules to be observed in the experiment. Due to AC-Stark shift during the excitation process electronic states which are not energetically accessible in the perturbative limit can be excited with high efficiency. Because dressed state selectivity is determined by phase jumps, the delay required to switch between different final states is in the order of half an optical cycle  $\Delta T/2 = \pi/\omega_0$ . Opposite to weak field spectral interference, the final population depends on the laser pulse intensity. Intensity dependent phase shifts of the selectivity – as observed in atoms [19] – are characteristic for SPODS.

Simple rules for the design of pulse sequences are derived from the insights into the physical mechanism of SPODS. Because phase changes during the pulse determine the selectivity of the dressed states population, shaped pulses with rapid changes of the temporal phase are employed. Sequences of two phase coherent pulses provide the simplest way to generate such phase jumps. Alternatively, by the use of a pulse shaper, sinusoidal phase modulation in frequency domain can be used to produce phase coherent pulse sequences [20,21]. The latter saves the efforts associated with an interferometric set-up and collinear alignment of the two beams. In terms of the laser intensity, the first pulse is tailored such that the pulse area is approximately  $\pi/2$  whereas the intensity of the second pulse is adapted to the required level shifts in the order of  $\mu\varepsilon = \hbar\Omega$ . In most cases – when significant level shifts are required – the second pulse is much more intense than the first one. Using low amplitudes of the sinusoidal spectral phase modulation function, this requirement is automatically fulfilled. The delay between these pulses is determined by two opposite requirements. On the one hand the whole sequence needs to be short enough to essentially freeze the vibrational motion because the selectivity decreases with increasing wave propagation time (cf. Fig. 4 at large delay times  $\tau$ ). Therefore the delay time  $\tau$  needs to be significantly shorter than the vibrational round trip time. On the other hand, in order to avoid (destructive) optical interference and to guarantee a well defined optical phase jump between both sub-pulses only partial overlap between both pulses is tolerable. Otherwise pulse energy is lost by (destructive) optical interference leading to reduced final population (cf. Fig. 4 at early delay times  $\tau$ ). Therefore the typical time delay between both sub-pulses is in the order of the pulse duration.

In this study, the influence of molecular rotation and the vectorial properties of the dipole moment was not investigated.

Molecular rotation during the excitation process is not a limitation of our scheme because rotation is frozen on the time scale of the laser pulses employed for SPODS. Because molecules will be generally found at random orientation in real samples, the efficiency of the population transfer might be lower in the experiment. The effect of random orientation could, for instance, be circumvented by rotational alignment prior to the SPODS-sequence [53]. Future simulations allowing for polarization shaping and including the effect of random molecular orientation, more electronic potentials and ionization will provide a more detailed picture of molecular quantum control via SPODS. The inclusion of energy resolved photoelectron spectra will be important to interpret experimental results obtained by photo-ionization.

## 5. Conclusion

In this wave packet study we extend strong field quantum control by selective population of dressed state as recently demonstrated experimentally on atoms to applications on real molecules. Simulations of the light-induced dynamics on the potential curves of the  $K_2$  dimer showed that efficient population transfer to a single predefined electronic state can be realized. High selectivity of about 80% is obtained in a two step process. In the first step a coherent superposition state of the electronic ground state and the first excited state is produced. By control of the relative temporal phase of a second pulse, the population of the intermediate dressed state is manipulated and transferred to a preselected final state via strong field induced resonance. In order to demonstrate that control is exerted by the relative phase between the two pulses, we studied the efficiency of the population transfer as a function of the delay between the two pulses. Comparison of the strong field results to weak field control emphasized that this physical mechanism is not based on common (multiphoton) weak field schemes such as spectral interference. In addition, light-induced level shifts in the order of  $2000\text{ cm}^{-1}$  made it possible to selectively populate even potentials that are energetically inaccessible in weak laser fields.

From these insights into the physical mechanism criteria for the design of efficient and highly selective pulse sequences were established in terms of pulse duration, intensity and phase relation. The required pulse sequence can be routinely produced in femtosecond labs because the pulse properties required for SPODS in terms of wavelength, pulse duration, intensity and interferometric control of the relative phase are readily obtained by standard equipment. Because switching among different final states is ultrafast, we believe that strong field quantum control via SPODS is applicable in the presence of decoherence channels as well. Because SPODS is ultrafast, robust and simple, we believe that strong field control via SPODS is generally applicable and at play in many other circumstances as well. Exploiting the vectorial properties of the dipole moment by combining strong laser fields with polarization shaping techniques promises a new level of quantum control. Experimental demonstrations of SPODS on alkali dimers and larger molecules are currently prepared in our labs.

## Acknowledgements

We would like to thank C. Meier and F. Spiegelman (Toulouse), for providing us with the electronic states and transition dipole moments used in this study. Financial support of the Deutsche Forschungsgemeinschaft is gratefully acknowledged.

## References

- [1] A.M. Weiner, Femtosecond pulse shaping using spatial light modulators, *Rev. Sci. Instrum.* 71 (5) (2000) 1929–1960.
- [2] A. Assion, T. Baumert, M. Bergt, T. Brixner, B. Kiefer, V. Seyfried, M. Strehle, G. Gerber, Control of chemical reactions by feedback-optimized phase-shaped femtosecond laser pulses, *Science* 282 (1998) 919–922.
- [3] H. Rabitz, R. de Vivie-Riedle, M. Motzkus, K. Kompa, Whither the future of controlling quantum phenomena? *Science* 288 (2000) 824–828.
- [4] S.A. Rice, M. Zhao, *Optical Control of Molecular Dynamics*, Wiley-Interscience, New York, 2000.
- [5] M. Shapiro, P. Brumer, *Principles of the Quantum Control of Molecular Processes*, Wiley-Interscience, Hoboken, 2003.
- [6] T. Brixner, T. Pfeifer, G. Gerber, M. Wollenhaupt, T. Baumert, in: P. Hannaford (Ed.), *Kluwer Series on Progress in Lasers: Femtosecond Laser Spectroscopy*, Springer, 2005, pp. 225–266 (Chapter 9: Optimal Control of Atomic, Molecular and Electron Dynamics with Tailored Femtosecond Laser Pulses).
- [7] M. Dantus, V.V. Lozovoy, Experimental coherent laser control of physicochemical processes, *Chem. Rev.* 104 (2004) 1813–1859.
- [8] T. Brixner, N.H. Damrauer, P. Niklaus, G. Gerber, Photosensitive adaptive femtosecond quantum control in the liquid phase, *Nature* 414 (2001) 57–60.
- [9] G. Vogt, G. Krampert, P. Niklaus, P. Nuernberger, G. Gerber, Optimal control of photoisomerization, *Phys. Rev. Lett.* 94 (2005) 068305-1–068305-4.
- [10] J.L. Herek, W. Wohlleben, R.J. Cogdell, D. Zeidler, M. Motzkus, Quantum control of energy flow in light harvesting, *Nature* 417 (2002) 533–535.
- [11] N.V. Vitanov, T. Halfmann, B.W. Shore, K. Bergmann, Laser-induced population transfer by adiabatic passage techniques, *Annu. Rev. Phys. Chem.* 52 (2001) 763–809.
- [12] M. Wollenhaupt, V. Engel, T. Baumert, Femtosecond laser photoelectron spectroscopy on atoms and small molecules: prototype studies in quantum control, *Annu. Rev. Phys. Chem.* 56 (2005) 25–56.
- [13] T. Frohnmeyer, M. Hofmann, M. Strehle, T. Baumert, Mapping molecular dynamics ( $\text{Na}_2$ ) in intense laser fields: another dimension to femtochemistry, *Chem. Phys. Lett.* 312 (5/6) (1999) 447–454.
- [14] J.G. Underwood, M. Spanner, M.Y. Ivanov, J. Mottershead, B.J. Sussman, A. Stolow, Switched wave packets: a route to nonperturbative quantum control, *Phys. Rev. Lett.* 90 (22) (2003) 223001-1–223001-4.
- [15] S.R. Hartmann, E.L. Hahn, Nuclear double resonance in the rotating frame, *Phys. Rev.* 128 (5) (1962) 2042–2053.
- [16] E.T. Sleva, I.M. Xavier Jr., A.H. Zewail, Photon locking, *J. Opt. Soc. Am. B* 3 (4) (1986) 483–487.
- [17] Y.S. Bai, A.G. Yodh, T.W. Mossberg, Selective excitation of dressed atomic states by use of phase-controlled optical fields, *Phys. Rev. Lett.* 55 (12) (1985) 1277–1280.
- [18] R. Kosloff, A.D. Hammerich, D. Tannor, Excitation without demolition: radiative excitation of ground-surface vibration by impulsive stimulated Raman scattering with damage control, *Phys. Rev. Lett.* 69 (15) (1992) 2172–2175.
- [19] M. Wollenhaupt, A. Assion, O. Bazhan, Ch. Horn, D. Liese, Ch. Sarpe-Tudoran, M. Winter, T. Baumert, Control of interferences in an Autler-Townes doublet: symmetry of control parameters, *Phys. Rev. A* 68 (2003) 015401-1–015401-4.
- [20] M. Wollenhaupt, A. Präkelt, C. Sarpe-Tudoran, D. Liese, T. Baumert, Quantum control and quantum control landscapes using intense shaped femtosecond pulses, *J. Mod. Opt.* 52 (16) (2005) 2187–2195.
- [21] M. Wollenhaupt, D. Liese, A. Präkelt, C. Sarpe-Tudoran, T. Baumert, Quantum control by ultrafast dressed states tailoring, *Chem. Phys. Lett.* 419 (2006) 184–190.
- [22] M. Wollenhaupt, A. Präkelt, C. Sarpe-Tudoran, D. Liese, T. Baumert, Quantum control by selective population of dressed states using intense chirped femtosecond laser pulses, *Appl. Phys. B* 82 (2006) 183–188.
- [23] M. Wollenhaupt, A. Präkelt, C. Sarpe-Tudoran, D. Liese, T. Baumert, Strong field quantum control by selective population of dressed states, *J. Opt. B: Topical issue on quantum control* 7 (2005) S270–S276.
- [24] M. Wollenhaupt, A. Assion, D. Liese, C. Sarpe-Tudoran, T. Baumert, S. Zamith, M.A. Bouchene, B. Girard, A. Flettner, U. Weichmann, G. Gerber, Interferences of ultrashort free electron wave packets, *Phys. Rev. Lett.* 89 (17) (2002) 173001-1–173001-4.
- [25] C. Meier, F. Spiegelman, private communication, 2005.
- [26] G. Jeung, Evaluation of the volume effect in the core–core interaction energy for alkali diatomics, *J. Mol. Spec.* 182 (1997) 113–117.
- [27] S. Magnier, Ph. Millié, Potential curves for the ground and numerous highly excited electronic states of  $\text{K}_2$  and  $\text{NaK}$ , *Phys. Rev. A* 54 (1) (1996) 204–218.
- [28] J.C. Barthelat, P. Durand, *Theor. Chim. Acta* 38 (1975) 283.
- [29] W. Müller, W. Meyer, Ground state properties of alkali dimers and their cations (including elements Li, Na, and K) from ab initio calculations with effective core polarization potentials, *J. Chem. Phys.* 80 (1984) 3311–3320.
- [30] S. Magnier, M. Aubert-Frécon, A.R. Allouche, Theoretical determination of highly excited states of  $\text{K}_2$  correlated adiabatically above  $\text{K}(4p) + \text{K}(4p)$ , *J. Chem. Phys.* 121 (4) (2004) 1771–1781.
- [31] H. Schwörer, R. Pausch, M. Heid, V. Engel, W. Kiefer, Femtosecond time-resolved two-photon ionization spectroscopy of  $\text{K}_2$ , *J. Chem. Phys.* 107 (23) (1997) 9749–9754.
- [32] M.A. Bouchene, V. Blanchet, C. Nicole, N. Melikechi, B. Girard, H. Ruppe, S. Rutz, E. Schreiber, L. Wöste, Temporal coherent control induced by wave packet interferences in one and two photon atomic transitions, *Eur. Phys. J. D* 2 (1998) 131–141.
- [33] M. Wollenhaupt, A. Assion, O. Bazhan, D. Liese, C. Sarpe-Tudoran, T. Baumert, One-parameter control of quantum dynamics using femtosecond pump-probe photoelectron spectroscopy on a model system, *Appl. Phys. B* 74 (1) (2002) S121–S125.
- [34] M. Wollenhaupt, A. Assion, O. Graefe, D. Liese, C. Sarpe-Tudoran, M. Winter, T. Baumert, Changes of the electronic structure along the internuclear coordinate studied by ultrafast photoelectron spectroscopy: the  $2^1\Sigma_u^+$   $\text{Na}_2$  double-minimum state, *Chem. Phys. Lett.* 376 (3/4) (2003) 457–464.
- [35] T. Brixner, G. Krampert, T. Pfeifer, R. Selle, G. Gerber, M. Wollenhaupt, O. Graefe, C. Horn, D. Liese, T. Baumert, Quantum control by ultrafast polarization shaping, *Phys. Rev. Lett.* 92 (20) (2004) 208301-1–208301-4.
- [36] M.D. Feit, J.A. Fleck Jr., Solution of the Schrödinger equation by a spectral method II: vibrational energy levels of triatomic molecules, *J. Chem. Phys.* 78 (1) (1983) 301–308.
- [37] A.J. Ross, P. Crozet, J. d’Incan, C. Effantin, The ground state,  $X^1\Sigma_g^+$ , of the potassium dimer, *J. Phys. B: At. Mol. Phys.* 19 (1986) L145–L148.
- [38] A.M. Lyyra, W.T. Luh, L. Li, H. Wang, W.C. Stwalley, The  $A^1\Sigma_u^+$  state of the potassium dimer, *J. Chem. Phys.* 92 (1) (1990) 43–50.
- [39] J.T. Kim, C.C. Tsai, W.C. Stwalley, The  $5^1\Sigma_g^+$  and  $6^1\Sigma_g^+$  states of  $^{39}\text{K}_2$  studied by optical–optical double resonance spectroscopy, *J. Mol. Spectrosc.* 171 (1995) 200–209.
- [40] J.T. Guoxing Zhao, J.T. Kim, W.C. Bahns, Stwalley, The  $2^1\Pi_g$  state of  $^{39}\text{K}_2$  studied by cw sub-doppler optical–optical double resonance spectroscopy, *J. Mol. Spectrosc.* 184 (1997) 209–214.
- [41] R. de Vivie-Riedle, K. Kobe, J. Manz, W. Meyer, B. Reischl, S. Rutz, E. Schreiber, L. Wöste, Femtosecond study of multiphoton ionization processes in  $\text{K}_2$ : from pump-probe to control, *J. Phys. Chem.* 100 (1996) 7789–7796.
- [42] C. Nicole, M.A. Bouchéne, C. Meier, S. Magnier, E. Schreiber, B. Girard, Competition of different ionization pathways in  $\text{K}_2$  studied by ultrafast pump-probe spectroscopy: a comparison between theory and experiment, *J. Chem. Phys.* 111 (17) (1999) 7857–7864.

- [43] A. Giusti-Suzor, F.H. Mies, L.F. DiMauro, E. Charron, B. Yang, Dynamics of  $H_2^+$  in intense laser fields, *J. Phys. B: At. Mol. Opt. Phys.* 28 (1995) 309–339.
- [44] B.M. Garraway, K.-A. Suominen, Adiabatic passage by light-induced potentials in molecules, *Phys. Rev. Lett.* 80 (5) (1998) 932–935.
- [45] I.R. Solá, B.Y. Chang, J. Santamaría, V.S. Malinovsky, J.L. Krause, Selective excitation of vibrational states by shaping of light-induced potentials, *Phys. Rev. Lett.* 85 (20) (2000) 4241–4244.
- [46] T. Baumert, V. Engel, C. Meier, G. Gerber, High laser field effects in multiphoton ionization of  $Na_2$ . Experiment and quantum calculations, *Chem. Phys. Lett.* 200 (5) (1992) 488–494.
- [47] V. Blanchet, C. Nicole, M.A. Bouchene, B. Girard, Temporal coherent control in two-photon transitions: from optical interferences to quantum interferences, *Phys. Rev. Lett.* 78 (14) (1997) 2716–2719.
- [48] D. Meshulach, Y. Silberberg, Coherent quantum control of two-photon transitions by a femtosecond laser pulse, *Nature* 396 (1998) 239–242.
- [49] A. Präkelt, M. Wollenhaupt, C. Sarpe-Tudoran, T. Baumert, Phase control of a two-photon transition with shaped femtosecond laser-pulse sequences, *Phys. Rev. A* 70 (2004) 063407-1–063407-10.
- [50] N.F. Scherer, R.J. Carlson, A. Matro, M. Du, A.J. Ruggiero, V. Romero-Rochin, J.A. Cina, G.R. Fleming, S.A. Rice, Fluorescence-detected wave packet interferometry: time resolved molecular spectroscopy with sequences of femtosecond phase-locked pulses, *J. Chem. Phys.* 95 (3) (1991) 1487–1511.
- [51] V. Blanchet, M.A. Bouchene, O. Cabrol, B. Girard, One-color coherent control in  $Cs_2$ . Observation of 2.7 fs beats in the ionization signal, *Chem. Phys. Lett.* 233 (1995) 491–499.
- [52] A.W. Albrecht, J.D. Hybl, S.M. Gallagher Faeder, D.M. Jonas, Experimental distinction between phase shifts and time delays: implications for femtosecond spectroscopy and coherent control of chemical reactions, *J. Chem. Phys.* 111 (24) (1999) 10934–10956.
- [53] H. Stapelfeldt, T. Seideman, Aligning molecules with strong laser pulses, *Rev. Mod. Phys.* 75 (2003) 543–558.